SPP1 targeted by miR-4262 in gastric cancer functions as an enhancer of cell growth and correlates with dismal prognosis

Junqing Wang (wangjunqingmd@hotmail.com)
Shanghai Institute of Digestive surgery https://orcid.org/0000-0001-6874-9614
Fengjie Hao
Department of Surgery, Ruijin Hospital, Shanghai Jiao Tong University School of Medicine
Yuchen Yang
Department of Surgery, Ruijin Hospital, Shanghai Jiao Tong University School of Medicine
Xiaochun Fei
Department of Pathology, Ruijin Hospital, Shanghai Jiao Tong University School of Medicine
Xunhua Chen
Department of Surgery, Ruijin Hospital, Shanghai Jiao Tong University School of Medicine

Primary research

Keywords: SPP1, gastric cancer, cell growth, miR-4262, post-transcriptional regulation

Posted Date: March 18th, 2020

DOI: https://doi.org/10.21203/rs.2.24820/v2

Abstract

Background Advanced gastric cancer (GC) induces diamal prognosis and high mortality. Discovery of new biomarkers or differentially expressed genes (DEGs) is serving for early diagnosis, prevention and therapautic treatmen in GC. In this study, by combining with biostatistics analysis, we aimed to verify the aberrant high expression and enhancing effects of SPP1 on GC, and to explore the probable relative post-transcriptional regulation. Methods Three datasets (GSE13911, GSE19826 and GSE27342) from NCBI GEO database were explored. SPP1 was screened out and detected in 105 real GC patients through immunohistochemistry analysis and RT-qPCR assay. The patients' clinicopathologic features were collected and analyzed. The expression of SPP1 was examinated in three GC cell lines (MKN-45, AGS and SNU-16) . MKN-45 cell model with SPP1 depletd was constrcted through shRNA transfection. CCK8 assay, cell cycle detection and apoptosis rate calculation were conducted to evaluate the ability of cell growth. MiR-4262 was filtered out as a potential up-streaming regulator of SPP1 mRNA through bioinformatic prediction, and the dual-luciferase reporter assay was used for validation. Rescue experiment was introduced to confirm the post-transcriptional regulation. Results Thirteen DEGs increased in GC were selected, among which SPP1 was screened out for its significant over-expression in GC. SPP1 expression profile was validated in both the 105 real GC patients' samples and three GC cell liens. High SPP1 expression was found significantly associated with the patients' clinicopathologic features related to unideal prognosis, including tumor size, lymph node metastasis, local invasion grade and TNM stage. Depletion of SPP1 remarkably suppressed the GC cell growth. Whilst, microRNA-4262 was validated directly binding to the 3'-UTR of SPP1 mRNA in GC cells, degenerating the expression of SPP1. Conclusions SPP1 probably functions as an oncogenic gene in GC, and provides us a new biomarker in GC hopeful to promote GC prevention, diagnose and therapeutic treatment.

Background

As one of the global health problem, gastric cancer (GC) results in the third leading cause of cancer-related death (1). Even though the improvements for GC treatment have been gradully achieved, the prognosis and over-all survival rate of the patients remain dismal (2).

The application of Gene Expression Omnibus (GEO) database from National Center for Biotechnology Information (NCBI) provides us possibility for intensive mining the differential expression genes (DEGs) involve in tumorigenesis. In this study, we set up an absolute value of fold-change (FC) of gene mRNA expression with a threshold criteria of $\log^2FC \geq 2.0$ and *P* value 1.0E-04, by which we clustered 13 DEGs amplified and 33 ones decreased from three NCBI GEO datasets (GSE13911, GSE19826 and GSE27342) (3-5). Among the candidates of the DEGs, we screened Secreted phosphoprotein 1 (SPP1) out of the 13 remarkably amplified DEGs for further study.

SPP1 was firstly reported concering in cell epitheial transformation process(6). Further studies then revealed SPP1 as a pivotal multi-functional genes participating in different processes intracellular, such as the attachment of osteoclasts to mineralized bone matrix (7), and up-regulation of IFN-γ and IL-12 through a cytokine way (8). Deregulation of SPP1, especially amplification in expression, has been reported in various human cancers, exerting critical effects on tumorigenesis and progress. For instance, high expressed SPP1 in epithelial ovarian cancer cells specifically activate Integrin-β/FAK/AKT pathway, and induces cell migration(9); up-regulated SPP1 in prostate cancer, SPP1 mediates the activity of Smad4/PTEN pathway and leads to tumor recurrence and metastasis (10). However, reports of the exact expression profile and the specific functions of SPP1 in GC are limited.

Thus, we detected and verified the pathological over-expression status of SPP1 in both the real GC patients' specimens and the GC cell lines. MKN-45 cell, one of the GC cell line highly expressing SPP1, was selected for the use of cell model construction. And depletion of SPP1 in the cell model further demonstrate suppressed characteristics of cell growth and mobility. Intriguingly, miR-4246 was detected as an upstream post-transcriptional regulator SPP1 through a classic miRNA modulated degeneration. All the aforementioned findings stongly suggest SPP1 as an effective enhancer in GC progress, which could be negatively regulated by miR-4262.

Materials And Methods

Gene expression profile data and the identification of DEGs

The gene expression datasets GSE11399, GSE19826 and GSE27342 were downloaded from GEO database (https://www.ncbi.nlm.nih.gov/geo/). Platforms of GEO datasets is GPL570 (Affymetrix Human Genome U133 Plus 2.0 Array) (Agilent Technologies, Santa Clara, CA, USA). There totally contains 130 cases of GC tumor tissues and 126 cases of non-cancerous gastric mucosa in the datasets for comparison.

Dataset with 55 GC tissues and 35 non-cancerous tissues from the Cancer Genome Altas (TCGA) database was obtained and was intensively explored to further validate the expression profile of the candidate DEGs (https://tcga-data.nci.nih.gov/tcga/).

R language, followed by normalization, was conducted by two professional bioinformatics analysts to preprocess the downloaded data, including background correction and transformation from probe level to gene symbol. DEGs differentiated between GC samples and non-cancerous tissues were defined basing on a *t*-test of linear models for microarray analysis package in R (Version 3.3, http://www.bioconductor.org) (11). A threshold criteria of $\log^2FC \geq 2.0$ and *P* value 1.0E-04 was set for DEG selection on gene expression FC calculated in this study. Funrich Software (Version 3.0, http://funrich.org/index.html) was utilized to analyze the DEGs overlapping characteristic among the three datasets.

The online database of Cancer Cell Line Encyclopedia (CCLE: https://portals.broadinstitute.org) was introduced for determining the gene expression status of the candidates among differential tumor cell lines.

The main data collected and processed from GEO, TCGA, CCLE and dbDEMC database was listed (Suppl. Table. 1).

Cell culture and surgical specimens,

The immortalized gastric epithelium cell line (GES-1) and three GC cell lines (MKN-45, AGS and SNU-16) were purchased from Shanghai Institutes for Biological Sciences, Chinese Academy of Science (Shanghai, China). RPMI 1640 supplemented with 10% heat-inactivated fetal bovine serum (FBS) (DPC, Tokyo, Japan) was used for cell culture in a humidified cell incubator, under the condition at 37℃ with an atmosphere of 5% CO_2, with 100 ug/ml streptomycin and 100U/ml Penicillin in the medium.

Specimens of the real GC patients conducted radical gastrectomy without preoperative therapy were recruited, including 105 paired tumor tissues and the adjacent non-cancerous tissues, at the Department of Surgery, Ruijin Hospital, Shanghai Jiao Tong University School of Medicine during 2017-2019. Ethical approval was granted by the research medical ethics committee of Ruijin Hospital, Shanghai Jiao Tong University School of Medicine.

Clinicopathologic features were collected and analyzed. And survival analysis of SPP1 was conducted by using online tool (http://www.kmplot.com) and Kaplan-Meier curves, including 876 GC patients with available clinical data.

Plasmid construction and transfection

MKN-45 cells in exponential phase were prepared and transfected with shRNA suppressing SPP1 mRNA translation through pGU6/Neo vectors (GenePharma, Shanghai, China) along with the construction of the control ones. Transfected cells were selected using medium mixed with G418 (Santa Cruz Biotechnology, Inc; 400 μg/ml).

Introduction of miR-4262 in MKN-45 cells (MKN-45/miR-4262) was carried out through mimic method similar to the description in our previous publication followed by the Dual-luciferase reporter assay (12, 13). And the control ones were setup simultaneously (NigmiR).

The RT-qPCR assay

Total RNA from cell lines was extracted by using TRIzol reagent (Invitrogen, USA). The first-strand cDNA was synthesized by using High-Capacity cDNA Reverse Transcription Kit (ABI, USA). RT-primers of OPN mRNAs were synthesized as follows: 5′- TCCTAGCCCCACAGACCCTT -3′ (forward) and 5′- CTGTGGAATTCACGGCTGAC -3′ (reverse) by Sangon Biotech Company (Shanghai, China). Real-time quantitative polymerase chain reaction (qRT-PCR) was conducted following the TaqMan Gene Expression Assays protocol (ABI, USA).

Immunohistochemistry assay and the Western blot analysis

Antibodies against SPP1 and GAPDH (Santa Cruz, USA) were prepared, along with horseradish peroxidase-conjugated secondary antibody (Abcam, USA). Immunohistochemistry (IHC) assay was conducted on paired tissues from the patients. SPP1 antibody was utilized as the manufactory instruction described (1:50), IgG antibody was used as control. Samples treated were then exammed by two professional pathologists blindly.

RIPA buffer containing Protease Inhibitor Cocktail (Pierce, USA) was prepared lysing cells. Concentration of the protein was measured \using BCA Protein Assay Kit (Pierce, USA). The extracted proteins were electrophoresed and electrotransfered. SPP1 antibody against (1:1000) and GAPDH (1:5000) were probed afterward. Horseradish peroxidase-conjugated secondary antibody was applied as further probe. GAPDH was regarded as the loading control.

Cell proliferation assay and cell cycle analysis

MKN-45 cells ($1x10^6$) stably transfected were cultured in 96-well microtiter plates in triplicate and incubated at 37˚C with an atmosphere of 5% CO_2 for 5 days. Microplate computer software (Bio-Rad Laboratories, Inc., Hercules, CA, USA) was used for measuring the OD following the Cell Counting Kit-8 (CCK-8) assay kit protocol (Dojindo, Tokyo, Japan). The cell proliferation curves were plotted.

The aforementioned cells were treated in steps with ethanol fixation, RNase A treatment and propidium iodide staining. Flow cytometry detection by using FACSCalibur (Becton-Dickinson, Franklin Lakes, NJ, USA) were conducted. Cell populations at the G0/G1, S and G2/M phases were quantified through ModFit software (Becton-Dickinson). Cell debris and fixation artifacts was excluded.

Cell apoptosis analysis

Cell apoptosis rate was calculated by using PE-Annexin V Apoptosis Detection Kit I (BD Pharmingen, USA) according to the product instructions. Stable transfected MKN-45 cells were resuspended in 1Î Binding Buffer ($1Î10^6$ cells/ml). 5μl of FITC and 5μl of PI were added into 100μl of cell suspension, followed by 15 minutes incubation in darkness and 400μlÎBinding Buffer was added. The analysis of apoptosis by flow cytometry (Becton Dickinson, USA) was conducted. Both Annexin V-FITC-positive and PI-negative cells were considered as apoptosis ones.

Verification of the degenerating effect of miR-4246 on SPP1 mRNA

Online database miRDB (http://mirdb.org) and TargetScan, (http://www.targetscan.org) were used for predicting potential miRNAs post-transcriptionally interacting with SPP1 mRNA. By intensively review manuscripts on pubmed (https://www.ncbi.nlm.nih.gov/pubmed/), we noticed miR-4262 is a probable post-transcriptional regulator of SPP1. The expression profile of miR-4262 was further verified among multiple human malignancies by using online tools from the Database of Differentially Expressed miRNAs in Human Cancers (dbDEMC, Version 2.0: http://www.picb.ac.cn/dbDEMC/) (Suppl. Table. 1).

A 202 bp sequence from the 3′-untranslated region (3′-UTR) of SPP1 mRNA covering the potential miR-4262 binding site was cloned into pMIR-REPORT luciferase vectors (Promega, USA), containing Firefly luciferase. The sequence was constructed as follow (Sangon Biotech Co., Shanghai, China): 5′-aauacaauuucucacuuugcauuuagucaaaagaaaaaaugcuuuauagcaaaaugaaagagaacaugaaaugcuucuuucucaguuuauugguugaaauguguaucuauuugagucuggaaauaac 3′. Correspondingly, the mutant sequence was transfected as follow: 5′-auuucuaauacacucauaggaauaacugauauguauauaagguauuuuggauauucauacacaucuucauaagguacauacacugauaaaucgaucauucucuuuguuuaucacugucguauuuag 3′. We used pRL-TK vectors containg Renilla luciferase as control. And MKN-45 cells either over-expressing miR-4262 or the negative control were co-transfected with vectors above. The luciferase activity was measured by Dual-Glo Luciferase assay system (Promega, USA) 48h post-transfection.

Statistics Analysis

Results derived and generated from specimens and cells were analyzed by using SPSS 18.0. Paired *t*-test and Fisher's exact test were considered statistically significant as *P* values < 0.05.

Results

Selection of the DEGs increased or decreased in GC

According to the criteria for DEGs selection of $\log^2$FC≥2.0 and *P* value＜1.0E-04, 464 genes increased in GC tissues were set compared with non-cancerous specimens. And, 1136 genes extremely decreased in GC tissues were selected simultaneously.

Among these genes, 46 genes were filtered out via FunRich software, among which 13 genes were over-expressed in tumor tissues, while the other 33 ones were decreased. Respectively, the 13 high expressed genes were HOXA13, SPP1, CST1, COL11A1, COL10A1, CLDN7, FNDC1, CLDN4, CLDN1, CHI3L1, CLDN3, CEMIP and SERPINB5（Fig. 1A）, and the 33 genes decreased were ATP4A, ATP4B, KCNE2, AQP4, GIF, LIPF, SULT2A1, KCNJ16, ADH7, CHIA, GKN1, GKN2, SOSTDC1, ESRRG, SST, FUT9, PDILT, FBP2, CPA2, PDIA2, CCKBR, MT1M, GHRL, CHGA, TFF2, PSCA, SCNN1G, C16orf89, KLK11, RDH12, AKR1B10, SCGB2A1, FGA (Fig. 1B). The expression fold-change of these DEGs, through TCGA database exploration and data mining, demonstrated extremely significant difference at mRNA status between tumor and normal gastric mucosa, partly illustrated in Fig. 1C.

In addition, as Suppl. Fig 1 and Suppl. Table.2 shown, GO and KEGG pathway enrichment analysis were carried out through online tools of the Database for Annotation Visualization and Integrated Discovery (DAVID, https://david.ncifcrf.gov/, Version 6.7) . The Search Tool for the Retrieval of Interacting Genes (STRING) database (Version 10.0, http://string-db.org) was applied for predicting the interaction between proteins derived from the DEGs. PPI network was estiblished through Cytoscape software (http://www.cytoscape.org/, Version 3.4.0).

SPP1 is highly expressed in GC tissues and cells, and is correlated with patients' survival status

According to the primary exploration of the GEO database, we screened SPP1 out of the 13 extremely highly expressed DGEs in GC tissues (*P*=2.58E-13 for GSE13911, *P*=8.32E-5 for GSE19826 and *P*=2.52E-10 for GSE27342) (Fig. 2A－C). In supplementary, we also analyzed the database of CCLE and observed the obvious inclination of high expression of SPP1 in different human malignancies including GC, and SPP1 presents a commonly incident up-regulation in multiple GC cell lines (Suppl. Fig. 2).

We detected the expression of SPP1 in three GC cell lines (MKN-45, AGS and SNU-16) through qRT-PCR assay and Western-blot analysis, and found SPP1was significantly increased in all the three GC cell lines compared with the control GES-1 cells (Fig. 2D, E) (*P*＜0.05).

The expression of SPP1 in 105 paired of specimens from GC patients was detected by IHC assay. SPP1 was verified highly expressed in 74.28% tumor tissues (78/105); and only 24.76% (26/105) samples of non-cancerous tissues present a relatively higher expression. Hence, the expression of SPP1 in tumor tissues was frequently and significantly higher than adjacent non-cancerous tissues (*P*＜0.01). (Fig. 3A, B)

Additionally, Kaplan-Meier plot was generated to indicate the correlation between SPP1 and patents' over-all survival (OS) or progression free survival rate (PFS). We collected 876 GC cases' follow-up information, and the generated OS and PFS data indicated that the patients' are significantly impaired when SPP1 was highly expressed (OS: HR=2.23, *P*=2.7E-14; PFS: HR=1.98, *P*=1.1E-10) (Fig. 3C).

High expression of SPP1 is associated with GC clinicopathologic features

The correlation between SPP1 expression status and the clinicopathologic features of the 105 GC cases was analyzed. As Table. 1 shown, there is no significant correlation between OPN expression and the patients' age, gender or tumor location. On the contrary, high expression of SPP1 inclines toward larger tumor size (P<0.05), more frequent lymph node metastasis (P<0.05), deeper local invasion (P<0.05), and more advanced TNM stages (P<0.05) in cases with higher SPP1 expression level, which indicates a doubtless correlation with SPP1 over-expression and a part of the GC clinicopathologic features.

SPP1 depletion suppresses cell proliferation, arrests the cell cycle and promotes cell apoptosis in MKN-45 cells

MKN-45 cells was found expressing the highest level of SPP1 among the three GC cell lines, and was selected and transfected with pGU6/Neo vectors for SPP1 effect. The effect of transfection was validated through RT-qPCR and Western blot analysis (Fig. 4A, B).

CCK8 assay was applied for evaluating the effect of SPP1 on GC cell proliferation. A significant suppression of cell proliferation in SPP1 depleted MKN-45 cells compared with the control MKN-45 cells, as P value<0.05 for d1, and P value<0.01 for d2 to d4 (Fig. 4C). Likewise, the flow cytometry analysis for cell cycle demonstrated that the cell cycle of MKN-45 cells was arrested at G0/G1 phase via SPP1 depletion (Fig. 4D, E). The percentage of MKN-45 cells in G0/G1 phase was raised from 46.29% to 64.78% (P<0.01); Cell portion distributing at S phase was decreased from 32.69% to 25.98%; and for G2/M phase, was decreased from 21.02% to 12.25%. Whilst, we also noticed an increased apoptosis rate of MKN-45 treated with SPP1 depletion, from 7.92% to 14.12% (P<0.01) (Fig. 4F, G).

All these results above indicate that SPP1 depletion significant defects the tumor cell growth in GC.

SPP1 is a post-transcriptionally targeted by miR-4262 in GC cells

MiRNAs are short non-coding RNAs consist of around 22 nucleotides, inducing post-transcriptional regulation of transcribed genes. By using online bioinformatics and prediction tools described in methods parts above, we found miR-4262, a miRNA aberrantly expressed in multiple human malignancies, is potentially function as the upstreaming modulator of SPP1 (Fig. 5A). Online software of dbDEMC (Version 2.0) indicates the expression of miR-4262 in human malignancies, which presents miR-4262 as a remarkably down-regulated miRNA in GC (Fig. 5B). On this basis, we detected the expression of miR-4262 in the three GC cell lines, and found that the expression of miR-4262 was significantly decreased in GC cells compared with GES-1 cells (P<0.01) (Fig. 5C).

The direct interaction between SPP1 mRNA and miR-4262 was detected via dual-luciferase reporter assay. As Fig 5D shown, luciferase signal for SPP1/pMIR/WT was significantly impaired when miR-4262 was introduced into MKN-45 cells (MKN-45/miR-4262). In contrast, this suppressive effect induced by miR-4262 could be remarkably abolished in MKN-45 cells with mutation of the putative miR-4262 binding site (SPP1/pMIR/MUT) (Fig. 5D). And the SPP1 expression at either mRNA status or protein status was significantly decreased in MKN-45/miR-4262 cells (Fig. 5E, F). These findings above suggest that SPP1 is one of the direct targets suppressed by miR-4262 in GC.

Re-upregulation of SPP1 in MKN-45 cells rescues the phenotype of cell growth and apoptosis induced by introducing miR-4262

In GC, miR-4262 had been verified significantly down-regulated in tumor tissues and cells, and plays a suppressive role in tumor progress, remarkably inhibiting the cell proliferation, and promotes the cell apoptosis (14).

Since we have validated the direct interaction between miR-4262 and SPP1 mRNA, we assumed that by re-introducing SPP1 into MKN-45 cells could rescue the phenotypes induced by miR-4262. In our study, we discovered that the suppressing function of miR-4262 of cell proliferation was significantly reversed by re-introducing SPP1 in MKN-45 cells (P value<0.05 for d1–d2, and P value<0.01 for d3–d4). Simultaneously, the cell cycle arrest and increase of cell apoptosis in MKN-45 cells were also partly rescued (Fig. 6).

Thus, we suggest that SPP1 is an enhancer of cell growth in GC, targeted by miR-4262.

Discussion

The tumorigenesis and progress of GC involves in multiple and complex mechanisms and molecules, such as mRNAs, noncoding RNAs and aberrant expressed proteins (15). Accumulating studies have reported a large amount of genes function in GC either promote or suppress the tumor process. As for the promotors, Cyclin Dependent Kinase 6 (CDK6) was reported significantly inducing cell invasion in GC (16); Plant homeodomain finger protein 10 (PHF10) promotes GC through enhancing cell proliferation (17); And, Solute carrier-7A5 (SLC7A5) and V-crk avian sarcoma virus CT10 oncogene homolog-like adapted protein of CRK family (CRKL) have been validated enhancing GC cell proliferation (18, 19). On the contrary, other genes were found playing suppressive or inhibiting roles in GC, and these genes commonly present decreased expression profiles in tumor tissues. For instance, EPB41L3 is a suppressor of GC cell invasion and migration, and is negatively regulated by miR-223 (20); Runt Related Transcription Factor 3 (RUNX3) is involved with transcription activity to suppress GC process, and is inactivated in GC cells by protein mis-localization (21); Moreover, the miR-338 targets SSX2IP is one contributing to the suppression induction of GC tumorigenesis (22).

Data mining for individual gene information via the datasets of NCBI GEO and TCGA databases could primarily give an integrative learning of the expression profiles and the relative functional network involved in GC process. In this study, we explored three GC patients' datasets of from the GEO database, which

totally included 130 GC samples and 126 non-cancerous gastric mucosa specimens for intensive analysis. By using $\log^2$FC=2.0 as the cut-off value, we observed 464 genes significantly increased in GC, and 1136 ones remarkably decreased, among tens of thousands of genes. We suppose to detect teh probable promotors or suppressors of GC among these candidates. The overlapped results from three individual datasets gave out two cohorts, inw which present 13 genes abnormally amplified and 33 genes decreased in tumor tissues.We observed that SPP1 was significantly increased in within the tumor tissues, and literatures and the GO and KEGG pathway analysis indicated SPP1 as an pivotal genes linked to several critical pathways close to tumor process, including integrin-mediated signaling pathway, extracellular matrix organization, cell-matrix adhesion and ECM-receptor interaction. Thus, SPP1 may probably affect GC process in an enhancing way.

SPP1 was originally reported involved in attachment of osteoclasts to the mineralized bone matrix (23). Evidence for the involvement of SPP1 in human malignancies indicates SPP1 as one of the promotors in multiple cancers. For instance, in colon cancer, SPP1 is highly expressed and significantly promotes tumor cell proliferation and angiogenesis (24); in non-small lung cancer, high expression of SPP1 induces tumor growth and enhances cell mobility (25). Recently, several studies have observed and suggested SPP1 as an indicator of the prognosis in GC(26-28). However, evidence of SPP1's promoting functions in GC is still limited.

In this study, our exploration indicated a common amplification of SPP1 expression from 105 paired real patients' tumor samples, and also three GC cell lines. Noticeably, survival analysis on either OS or PFS in GC patients demonstrated significant poor outcome of the patients with higher SPP1 expression. Meanwhile, we co-analyzed the SPP1 expression status and GC patients' clinicopathologic features. We discovered that high SPP1 expression is significantly correlated with some of the parameters dismal in prognosis, especially the larger tumor size, higher local invasion degree, severer lymphnode metastasis and more advanced tumor stages. Considering the findings above, we further focused and detected the effect of SPP1 on GC tumors growth. As we supposed, the depletion of SPP1 significantly arrested the cell cycles of GC cells and impaired the ability of cell proliferation. And in accordance with these, SPP1 also induced significant cell apoptosis in MKN-45 cells. Thus we regard SPP1 as a biomarker indicating GC tumor progress and poor prognosis, enhancing the cell growth of tumor.

Specific cellular mechanisms are involved with the regulation of the signature genes or biomarkers in tumor. As acknowledged, miRNAs, which are transcripts with non-coding characteristics composed with around 22 nucleotides, are a kind of upstreaming regulators involves in tumor process suppressing or degenerating target mRNAs (29, 30). We supposed post-transcriptional regulation upstreaming SPP1 plays critical role in GC process.

By using bioinformatics prediction, we found miR-4262 is a potential upstreaming probably binding to the 3'UTR of SPP1 mRNA. According to the reports and literatures, miR-4262 is a yet validated non-coding molecule participating in multiple processes either promoting or suppressing tumorigenesis. For example, in hepatocellular carcinoma, miR-4262 negatively regulates PDCD4 and then induces activation of NF-κB pathway, causing tumor cell proliferation (31); In acute myeloid leukemia, high expression of miR-4262 is found in both bone marrow and patients' serum, which is associated with short survival period and poor prognosis (32). On the contrary, miR-4262 acts as an important suppressor in cervical cancer by directly degenerating mRNA of ZETB33, and impacts cell proliferation and EMT process (33). Recent report has pointed out that miR-4262 expression is significantly decreased in GC cells, and exerts suppressive effects cell growth by targeting proto-oncogene CD163, along with the promotion of cell apoptosis (14).

In our study, the significant down-regulation of miR-4262 in GC cells through qRT-PCR assay was validated compared with GES-1 cells. Then, we conducted the dual-luciferase reporter assay in the MKN-45 cell models ectopically expressing miR-4262. Remarkably deduction of luciferase signal was observed when the binding site was mutated, and the expression of SPP1 was consequently impaired after miR-4262 introduction, which indicates an exact direct regulation of SPP1 in GC cells modulated by miR-4262. Simultaneously, the rescue experiment confirmed the reversion of the impact of miR-4262 suppressing the cell proliferation, which further supports the inhibiting effect of miR-4262 on GC cell growth via degenerating SPP1.

Conclusion

In summary, we found high expression of SPP1 in GC is significantly correlated with the dismal parameters of the clinicopathologic features, and is relative with poor prognosis. Depletion of SPP1 in vitro, could remarkably suppress GC cell growth. And miR-4262 functions as the post-transcriptional regulator upstreaming OPN. And OPN is hopefully a new biomarker for GC, indicating advanced tumor stages and poor prognosis.

List Of Abbreviations

GC: gastric cancer; DEGs: differentially expressed genes; GEO: Gene Expression Omnibus database; NCBI: National Center for Biotechnology Information; TCGA: the Cancer Genome Altas; FC: fold-change; SPP1: Secreted phosphoprotein 1; CCLE: The online database of Cancer Cell Line Encyclopedia; GES-1: the immortalized gastric epithelium cell line; FBS: fetal bovine serum; miRNA: microRNA; RT-qPCR: quantitative real-time polymerase chain reaction; shRNA: short hairpin RNA. CCK8: the Cell Counting Kit-8; 3'-UTR: the 3'-untranslated region;

Declarations

Ethics approval and consent to participate

Informed consent was obtained and the study was approved by the Ethics Committee of Ruijin Hospital, Shanghai Jiaotong University School of Medicine, in accordance with the Declaration of Helsinki.

Consent for publication

The individual personal data in this study could be used for publication with the consents.

Availability of data and material

All data obtained in this study is included in this published article and its supplementary materials.

Competing interests

No potential competing interest was disclosed.

Funding

This study was kindly supported by grants from the following: National Natural Science Foundation of China (No. 81602544); Shanghai Pujiang Talent Project (No. 18PJD029); Research physician project from Shanghai Jiao Tong University School of Medicine (20191901).

Authors' contributions

Junqing Wang managed the project and the experiments in this study; Xiaochun Fei was in charge of the pathological examination; Yuchen Yang contributed for the data analysis; Fengjie Hao participated in the bio-molecular experiment and the wet lab job; Xuehua Chen contributed for the direction of this project.

Acknowledgements

The authors thank Shen Chen, Di Ma, Ye Lu, Xiaoyong Gong and Jiajun Ren for providing valuable technical supports and assistance.

References

1. Thrift AP, El-Serag HB. Burden of Gastric Cancer. Clinical gastroenterology and hepatology : the official clinical practice journal of the American Gastroenterological Association. 2019.
2. Katona BW, Rustgi AK. Gastric Cancer Genomics: Advances and Future Directions. Cell Mol Gastroenterol Hepatol. 2017;3(2):211-7.
3. Cui J, Chen Y, Chou WC, Sun L, Chen L, Suo J, et al. An integrated transcriptomic and computational analysis for biomarker identification in gastric cancer. Nucleic acids research. 2011;39(4):1197-207.
4. Wang Q, Wen YG, Li DP, Xia J, Zhou CZ, Yan DW, et al. Upregulated INHBA expression is associated with poor survival in gastric cancer. Med Oncol. 2012;29(1):77-83.
5. Cho JY, Lim JY, Cheong JH, Park YY, Yoon SL, Kim SM, et al. Gene expression signature-based prognostic risk score in gastric cancer. Clinical cancer research : an official journal of the American Association for Cancer Research. 2011;17(7):1850-7.
6. Han X, Wang W, He J, Jiang L, Li X. Osteopontin as a biomarker for osteosarcoma therapy and prognosis. Oncol Lett. 2019;17(3):2592-8.
7. Fraher D, Hodge JM, Collier FM, McMillan JS, Kennedy RL, Ellis M, et al. Citalopram and sertraline exposure compromises embryonic bone development. Mol Psychiatry. 2016;21(5):656-64.
8. Kashani-Sabet M, Nosrati M, Miller JR, 3rd, Sagebiel RW, Leong SPL, Lesniak A, et al. Prospective Validation of Molecular Prognostic Markers in Cutaneous Melanoma: A Correlative Analysis of E1690. Clinical cancer research : an official journal of the American Association for Cancer Research. 2017;23(22):6888-92.
9. Zeng B, Zhou M, Wu H, Xiong Z. SPP1 promotes ovarian cancer progression via Integrin beta1/FAK/AKT signaling pathway. OncoTargets and therapy. 2018;11:1333-43.
10. Ding Z, Wu CJ, Chu GC, Xiao Y, Ho D, Zhang J, et al. SMAD4-dependent barrier constrains prostate cancer growth and metastatic progression. Nature. 2011;470(7333):269-73.
11. Love MI, Huber W, Anders S. Moderated estimation of fold change and dispersion for RNA-seq data with DESeq2. Genome Biol. 2014;15(12):550.
12. Feng R, Chen X, Yu Y, Su L, Yu B, Li J, et al. miR-126 functions as a tumour suppressor in human gastric cancer. Cancer Lett. 2010;298(1):50-63.
13. Wang J, Chen X, Li P, Su L, Yu B, Cai Q, et al. CRKL promotes cell proliferation in gastric cancer and is negatively regulated by miR-126. Chem Biol Interact. 2013;206(2):230-8.
14. Zhang H, Jiang H, Zhang H, Liu J, Hu X, Chen L. miR-4262, low level of which predicts poor prognosis, targets proto-oncogene CD163 to suppress cell proliferation and invasion in gastric cancer. OncoTargets and therapy. 2019;12:599-607.
15. Bringeland EA, Wasmuth HH, Fougner R, Mjones P, Gronbech JE. Impact of perioperative chemotherapy on oncological outcomes after gastric cancer surgery. Br J Surg. 2014.
16. Feng L, Xie Y, Zhang H, Wu Y. miR-107 targets cyclin-dependent kinase 6 expression, induces cell cycle G1 arrest and inhibits invasion in gastric cancer cells. Medical oncology. 2012;29(2):856-63.
17. Wet M, Liu JY, Lv X, Nei H, Liu BY, Zhu ZG, et al. [Preparation of PHF10 antibody and analysis of PHF10 expression gastric cancer tissues]. Xi bao yu fen zi mian yi xue za zhi = Chinese journal of cellular and molecular immunology. 2010;26(9):874-6.
18. Wang J, Chen X, Su L, Li P, Cai Q, Liu B, et al. MicroRNA-126 inhibits cell proliferation in gastric cancer by targeting LAT-1. Biomedicine & pharmacotherapy = Biomedecine & pharmacotherapie. 2015;72:66-73.
19. Wang J, Chen X, Su L, Li P, Liu B, Zhu Z. LAT-1 functions as a promotor in gastric cancer associated with clinicopathologic features. Biomedicine & pharmacotherapy = Biomedecine & pharmacotherapie. 2013;67(8):693-9.

20. Li X, Zhang Y, Zhang H, Liu X, Gong T, Li M, et al. miRNA-223 promotes gastric cancer invasion and metastasis by targeting tumor suppressor EPB41L3. Mol Cancer Res. 2011;9(7):824-33.
21. Ito K, Liu Q, Salto-Tellez M, Yano T, Tada K, Ida H, et al. RUNX3, a novel tumor suppressor, is frequently inactivated in gastric cancer by protein mislocalization. Cancer Res. 2005;65(17):7743-50.
22. Li P, Chen X, Su L, Li C, Zhi Q, Yu B, et al. Epigenetic silencing of miR-338-3p contributes to tumorigenicity in gastric cancer by targeting SSX2IP. PloS one. 2013;8(6):e66782.
23. Ozeki N, Mogi M, Hase N, Hiyama T, Yamaguchi H, Kawai R, et al. Polyphosphate-induced matrix metalloproteinase-13 is required for osteoblast-like cell differentiation in human adipose tissue derived mesenchymal stem cells. Biosci Trends. 2016;10(5):365-71.
24. Chu CM, Yao CT, Chang YT, Chou HL, Chou YC, Chen KH, et al. Gene expression profiling of colorectal tumors and normal mucosa by microarrays meta-analysis using prediction analysis of microarray, artificial neural network, classification, and regression trees. Dis Markers. 2014;2014:634123.
25. Shojaei F, Scott N, Kang X, Lappin PB, Fitzgerald AA, Karlicek S, et al. Osteopontin induces growth of metastatic tumors in a preclinical model of non-small lung cancer. J Exp Clin Cancer Res. 2012;31:26.
26. Zhuo C, Li X, Zhuang H, Tian S, Cui H, Jiang R, et al. Elevated THBS2, COL1A2, and SPP1 Expression Levels as Predictors of Gastric Cancer Prognosis. Cell Physiol Biochem. 2016;40(6):1316-24.
27. Lee SH, Park JW, Go DM, Kim HK, Kwon HJ, Han SU, et al. Ablation of osteopontin suppresses N-methyl-N-nitrosourea and Helicobacter pylori-induced gastric cancer development in mice. Carcinogenesis. 2015;36(12):1550-60.
28. Jin Y, Da W. Screening of key genes in gastric cancer with DNA microarray analysis. Eur J Med Res. 2013;18:37.
29. Kiselev FL. [MicroRNA and cancer]. Molekuliarnaia biologiia. 2014;48(2):232-42.
30. Wang J, Zhou Y, Fei X, Chen X, Zhu Z. Regulator of G-protein signaling 3 targeted by miR-126 correlates with poor prognosis in gastric cancer patients. Anti-cancer drugs. 2016.
31. Lu S, Wu J, Gao Y, Han G, Ding W, Huang X. MicroRNA-4262 activates the NF-kappaB and enhances the proliferation of hepatocellular carcinoma cells. International journal of biological macromolecules. 2016;86:43-9.
32. Han GT, Sun ZL. Up-regulation of serum miR-4262 predicts clinical outcome of patients with acute myeloid leukemia. European review for medical and pharmacological sciences. 2017;21(9):2172-6.
33. Feng J. Upregulation of MicroRNA-4262 Targets Kaiso (ZBTB33) to Inhibit the Proliferation and EMT of Cervical Cancer Cells. Oncology research. 2018;26(8):1215-25.

Figures

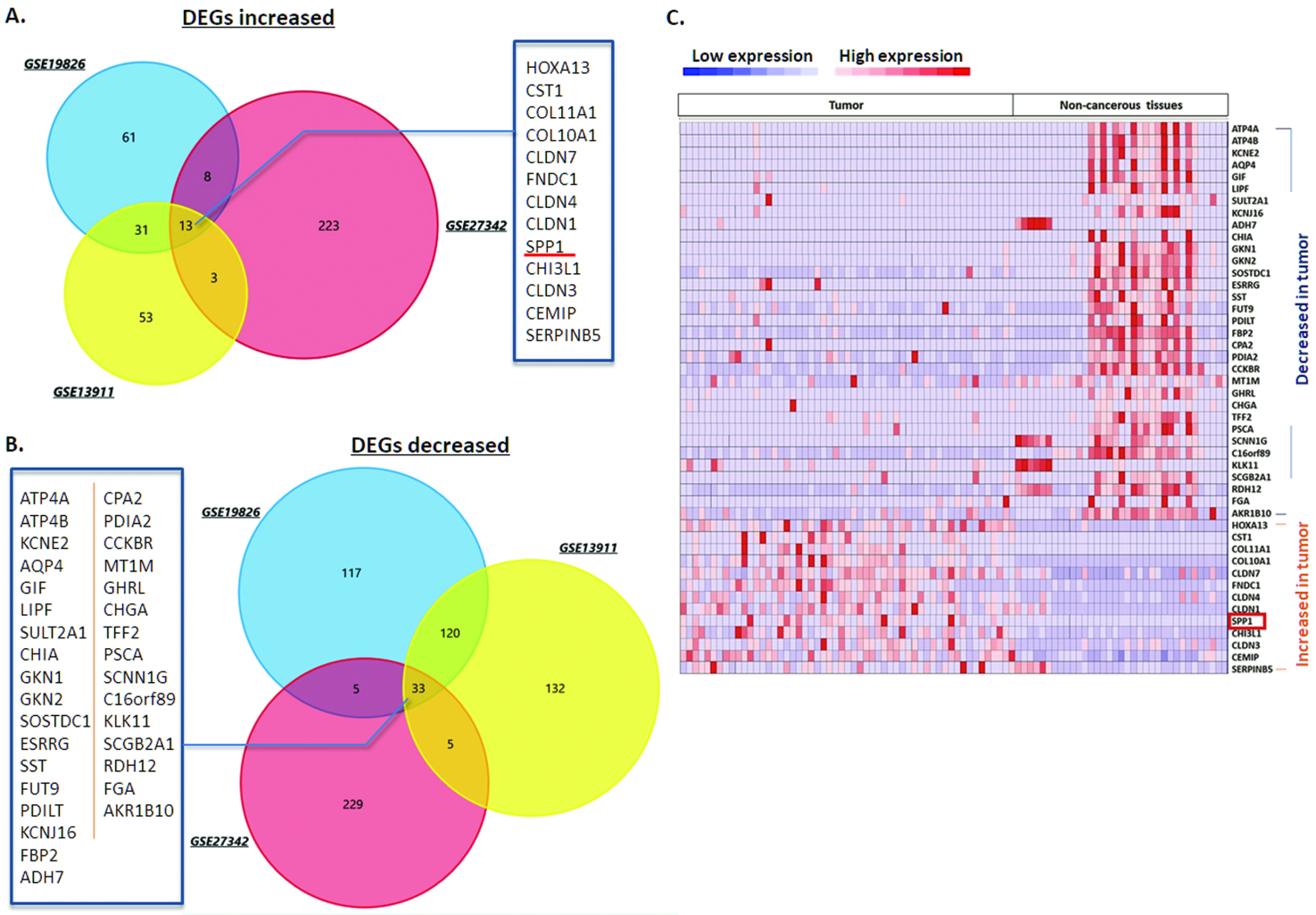

Figure 1

DEGs selection from NCBI GEO and TCGA database A. Venn chart of the increased genes in GSE13911, GSE19826 and GSE27342 datasets. Thirteen DEGs over-expressed in the three datasets were selected. B. Venn chart of the decreased genes in the NCBI GEO datasets above. Thirty-three DEGs were selected from the three datasets. C. Heatmap generated from TCGA database for GC. The bar indicates the relative expression level of separate genes in differential samples, from blue to red, which indicates low expression of gene mRNAs to high expressed ones.

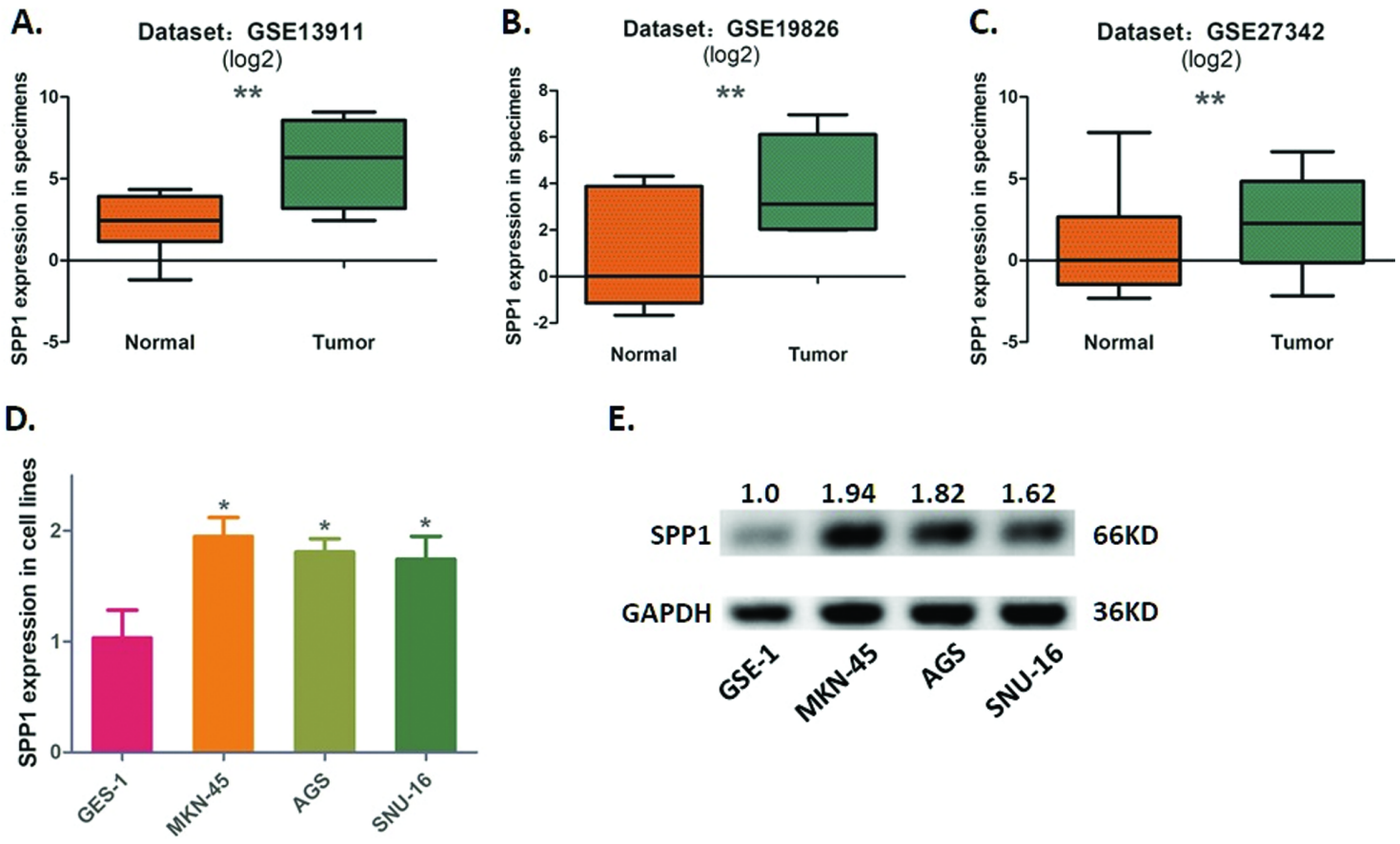

Figure 2

SPP1 expression profile of NCBI GEO datasets analysis and GC cell lines A□C. Comparison of SPP1 mRNA levels between GC tumor and non-cancerous tissues from GEO datasets. SPP1 presents significantly higher expression in tumor tissues, respectively in GSE13911 (**P=2.58E-13); GSE19826 (**P=8.32E-5) and GSE27342 datasets (**P=2.52E-10). C. RT-q PCR assay for detecting the mRNA expression of SPP1 in three GC cell lines (MKN-45, AGS and SNU-16). SPP1 mRNA is highly expressed in three GC cell lines compared with the control GES-1 cells (*P□0.05). D. The Western blot analysis for detecting the protein expression of SPP1 in three GC cell lines. SPP1 protein is highly expressed in these three GC cell lines compared with GES-1 cells.

Figure 3

Expression profile of SPP1 in specimens, and analysis of patients' OS and PFS according to the follow-up information A. Statistic of number of cases with higher or lower expression of SPP1 in specimens. SPP1 was up-regulated in most of the tumor tissues (78/105), and was expressed at a lower level in most of the adjacent non-cancerous tissues (79/105). (P□0.01). B. Representative graph of immunohistochemistry analysis (400×). Specimens stained IgG anti-body were regarded as control. SPP1 expression in GC tumor specimens was significantly higher than in adjacent non-cancerous tissues. C. Over-all survival (OS) and progression free survival (PFS) analysis according to GC patients' follow-up information was conducted and presented by Kaplan-Meier plot. High SPP1 level in GC tissue is correlated poor OS (876 cases, P=2.7E-14) and poor PSF (641 cases, P=1.1E-10).

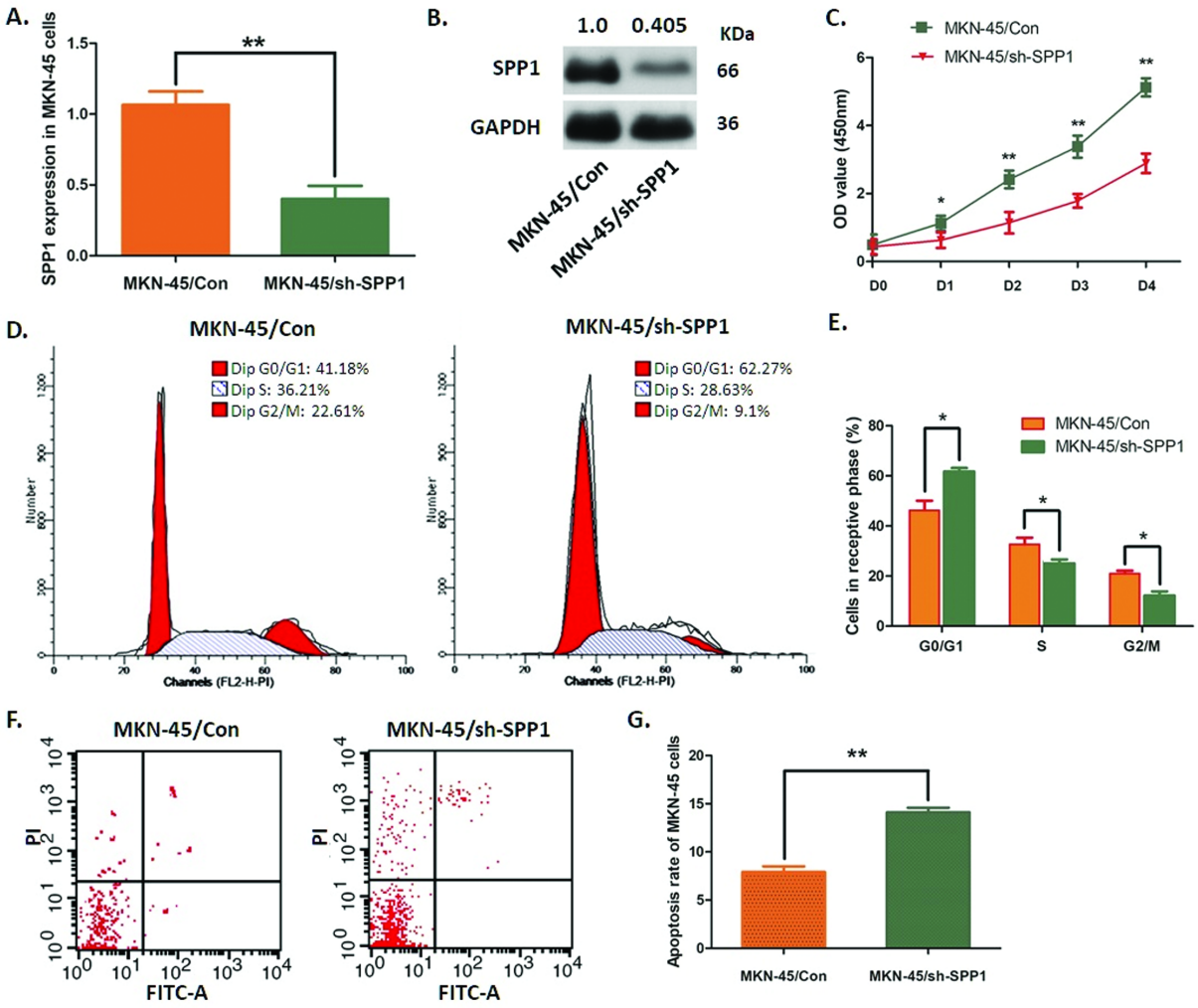

Figure 4

SPP1 depletion suppresses cell proliferation, arrests the cell cycle and promotes cell apoptosis in MKN-45 cells A. SPP1 depletion was conducted in MKN-45 cells by using shRNA transfection. RT-qPCR assay indicated a significant defection of SPP1 mRNA expression in the treated cells (**P< 0.01). B. The Western blot analysis was carried out and validated the significant reduction of SPP1 protein in MKN-45 cells by SPP1 depletion treatment. C. CCK8 assay was applied for detection of effect of SPP1 on cell proliferation. The MKN-45 cell proliferation was significantly impaired by depleting SPP1 (*P< 0.05, **P< 0.01). D–E. Flow cytometry was utilized for analysis of the cell cycle. The representative histograms describing cell cycle profiles of MKN-45 cells are shown. The cell cycle of MKN-45 cells was significantly arrested in G0/G1 phase by depleting SPP1. The results are means of three independent experiments ±SD. (*P< 0.05). F–G. Cell apoptosis was detected by flow cytometry. The representative histograms describing cell apoptosis profile in MKN-45 cells are shown. The apoptosis rate of MKN-45 cells was significantly increased from 7.92% to 14.12% via SPP1 depletion. The results are means of three independent experiments ±SD. (**P< 0.01).

Figure 5

MiR-4262 directly regulates SPP1 expression in MKN-45 cells post-transcriptionally A. Predicted binding site in the wild type SOX4 mRNA 3′-UTR (WT-UTR) with the seed sequence of miR-4262. The minimum free energy (Mfe) hybridization is calculated as: -17.7kal/mol. B. Expression profile of miR-4262 in multiple human malignancies. MiR-4262 is significantly decreased in GC tumor tissues compared with the normal stomach mocusa. C. RT-qPCR assay indicated that miR-4262 was down-regulated in multiple GC cell lines compared with the control GES-1 cells (**P<0.01). D. The direct binding between miR-4263 and SPP1 was detected by Dual-luciferase reporter assay. Up-regulation miR-4262 through mimics in MKN-45 cells (MKN-45/miR-4262) decreased the luciferase signal of SPP1/pMIR/WT significantly in cells with compared with the negative control (MKN-45/miR-4262) , while mutation of the putative miR-4262-binding site abolished this suppressive effect (**P<0.01). E. RT-qPCR assay indicated a significant decrease of SPP1 mRNA expression in MKN-45 cells treated with miR-4262 up-regulation (**P<0.01). F. The Western blot analysis indicated a significant decrease of SPP1 protein expression in MKN-45 cells treated with miR-4262 up-regulation.

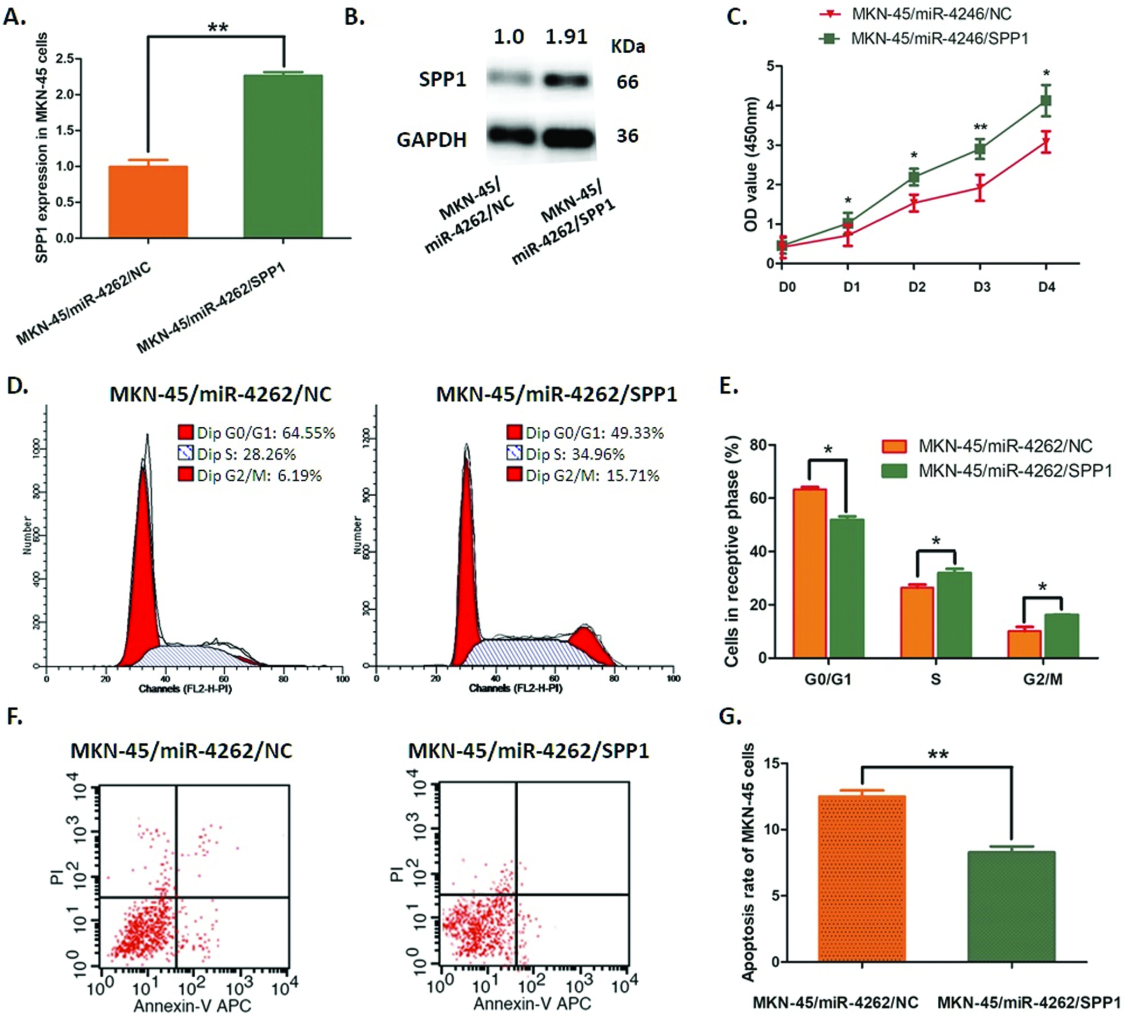

Figure 6

Re-upregulation of SPP1 in MKN-45 cells rescues the phenotype of cell growth and apoptosis induced by introducing miR-4262 A□B. The effect of re-upregulation of SPP1 in MKN-45 cells at both mRNA and protein levels was validated respectively through RT-qPCR assay and the Western blot analysis (**P□ 0.01). C. Cell proliferation was detected by CCK8 assay. Re-introducing SPP1 significantly rescued the suppression of cell proliferation induced by miR-4262 in MKN-45 cells (*P□0.05, **P□0.01). D□E. The representative histograms describing cell cycle profiles of MKN-45 cells are shown calculated by using flow cytometry. The cell cycle arrest of MKN-45 cells was significantly rescued via re-introducing SPP1, and the cell count of G0/G1 phase was remarkably reduced. The results are means of three independent experiments ±SD. (*P< 0.05). F□G. Cell apoptosis rate was calculated by flow cytometry. The increased apoptosis rate of MKN-45 cells induced by miR-4262 was significantly reduced from via re-introducing SPP1. The results are means of three independent experiments ±SD. (**P< 0.01).

Supplementary Files

This is a list of supplementary files associated with this preprint. Click to download.

- Suppl.Table.1revised.xlsx
- SupplFigures.docx
- Suppl.Table.2revised.docx